



A Graphene Oxide Nanoprobe for Sensitive Fluorescent Telomerase Activity Analysis

**Bin Zhu¹, Ruiguo Cao¹, Yuanyuan Jiang¹, Qi Li¹, Qiang Zhang¹,
Gu Yuan¹, Jingjian Li^{1*} and Dongsheng Xu^{1*}**

¹*Beijing National Laboratory for Molecular Sciences, College of Chemistry and Molecular Engineering, Peking University, Beijing 100871, P. R. China.*

Authors' contributions

This work was carried out in collaboration between all authors. Authors JL and DX designed the study. Author BZ and RC performed the entire experiment work. Author BZ wrote the first draft of the manuscript. Authors YJ and QL analysed the graphene oxide by Raman. Authors QZ and GY managed the electrophoretic analyses of the study. All authors read and approved the final manuscript.

Article Information

DOI: 10.9734/IRJPAC/2014/12197

Editor(s):

(1) Francisco Marquez-Linares, Full Professor of Chemistry, Nanomaterials Research Group School of Science and Technology, University of Turabo, USA.

Reviewers:

(1) Anonymous, National Institute for Material Science, Netherlands.

(2) Anonymous, Amity University, Up, India.

(3) Grigoriy Sereda, Chemistry Department, University of South Dakota, USA.

Peer review History: <http://www.sciencedomain.org/review-history.php?iid=536&id=7&aid=5890>

Original Research Article

Received 22nd June 2014
Accepted 9th August 2014
Published 25th August 2014

ABSTRACT

A novel fluorescent biosensor with ultra-sensitivity and selectivity for telomerase detection has been designed based on oligonucleotide-adsorption to graphene oxide (GO). This PCR-free method employs fluorescent ssDNA as a probe, which exhibits minimal background fluorescence in the presence of GO. In the test procedure, telomeric primer DNA was incubated with cancer cell extract and dNTP molecules for 18 hours and then

*Corresponding author: Email: lijj@pku.edu.cn;

added to the fluorescent probe solution. If telomerase is present and active, this telomeric primer will be elongated and hybridised with the fluorescent DNA probe, causing strong fluorescence emission due to the formation of double helix DNA and its detachment from the surface of GO. If telomerase is absent or inactive (e.g. due to heating in the incubation solution), the telomeric primer will not be elongated, preventing hybridisation with the fluorescent DNA probe. Therefore, in the absence of telomerase, fluorescence is quenched by GO, enabling detection of telomerase activity with a high signal-to-background ratio. Using this GO-based fluorescence method, the telomerase activity detection limits were 5 cells and 50 cells under $0.2 \text{ mg}\cdot\text{mL}^{-1}$ and $0.5 \text{ mg}\cdot\text{mL}^{-1}$ GO concentration, respectively.

Keywords: Graphene oxide; telomerase activity; fluorescent probe; ultra-sensitivity.

1. INTRODUCTION

Telomerase is an essential cellular ribonucleoprotein (RNP) that stabilises telomere length by adding TTAGGG repeats onto the telomeric ends of the chromosomes using reverse transcription and intrinsic RNA as a template [1-4]. Over 85% of all known human tumours exhibit high telomerase activity compared to neighbouring normal cells. Therefore, it is regarded as a biomarker for cancer diagnosis as well as a therapeutic target [5-7]. To date, many telomerase analysis protocols have been developed, including the telomeric repeat extension protocol [8], telomeric repeat amplification protocol (TRAP) [9], homogeneous chemiluminescent assay (HPA) [10], RT-PCR analysis of human telomerase reverse transcriptase (hTERT) gene expression [11] and rolling-circle mechanism telomeric arrays (RCA) [12]. Among these methods, polymerase chain reaction (PCR)-based TRAP is the most sensitive and widely-used telomerase activity detection assay. Although powerful, TRAP is limited by its requirement for expensive equipment and reagents, such as PCR instrumentation and Taq polymerases. In addition, it is susceptible to PCR-derived artefacts, especially when screening compounds for telomerase inhibition. Furthermore, the exponential amplification of products increases the risk of false positives and complicates the accurate quantification of telomerase activity [13]. In the last decade, the advancement of nanotechnologies has facilitated the development of many other methods for detecting telomerase activity [14, 15]. These methods include colorimetric detection by DNAzyme [16, 17], quartz crystal microbalance methods [18], electrical and surface plasmon resonance methods [19,20] chemiluminescence [21] and electrochemiluminescence methods [22] based on nanoprobe, electrochemical impedance spectroscopy (EIS) [23], electrochemical methods by using a ligands bound to tetraplex DNA [24] as well as using Au nanoparticles amplification means [25]. These new methods are PCR-free and most of them incorporate nanoscale elements. Moreover, in addition to consider the DNA extension in TRAP, these new methods still maintained the unique composition and structure of telomeric repeat sequences. However, the sensitivity of these methods is usually insufficient without amplification by PCR process. (See supplementary Data Table S1.).

Herein, we report a novel method to detect telomerase activity using a sensitive fluorescent probe based on DNA-adsorption to graphene oxide. Graphene consists of a single layer of carbon atoms in a closely-packed, honeycomb two-dimensional lattice and possesses exceptional electronic properties and enormous potential for applications. It has been actively studied as a chemical sensor material since 2004, when it was first isolated [26-31]. In recent years, it has shown particular promise as a component in biotechnology

applications such as DNA sequencing [32]. Yang et al. [33] and Fan et al. [34] independently proposed that water-soluble graphene oxide (GO) could selectively adsorb single stranded DNA (ssDNA) probes. This strong adsorption of ssDNA was attributed to the π - π stacking interaction between the ring structures in nucleobases and the hexagonal cells of graphene. In their work, a graphene oxide (GO)-based multicolour fluorescent DNA nanoprobe was reported. Due to the high signal-to-background ratio between ssDNA and dsDNA with GO, this nanoprobe allowed rapid, sensitive, and selective detection of DNA targets in homogeneous solution. Utilising this low cost unique multifunctional material, they detected various target molecules, such as target DNA, Hg^{2+} , Ag^+ , and ATP [35]. Willner et al. also developed multiplexed aptasensors and amplified DNA detection based on the functional GO by coupling exonuclease III, Exo III, to system, and applied it into logic gate operation [36]. Using the extraordinarily high quenching efficiency of GO, we developed a PCR-free assay for telomerase activity detection based on the conformational change of a DNA probe from single strand to double helix after elongation by telomerase. This new assay achieves higher sensitivity than the TRAP method.

2. EXPERIMENT SECTION

2.1 Chemicals and Materials

Water-soluble graphene oxide (GO) was synthesised using the chemical Hummers method [37-39]. The GO product was dialysed in distilled water to completely remove metal ions and acids. After centrifugation for 10 min at 8000 rpm, the supernatants containing GO were collected and brought to a concentration of 1 mg/mL.

Two kinds of polyacrylamide gel electrophoresis (PAGE) -purified DNA fragments were used for telomerase activity detection, both of which were synthesised and provided by Sangon. Co. Ltd. (Shanghai, China). The sequences were as follows: P1: 5'-CCCTAACCCCTAACCCCTAACCCCTAACTC-FAM-3' (27 bp); P2: 5'-AATCCGTCGAGCAGAGTT-3' (18 bp). The P1 sequence was used as the fluorescent probe with a complementary sequence to the telomeric repeat sequence, while P2 was the telomerase primer. All these probes and primers were prepared as a 1 μ M concentration in 20 mM Tris-HCl buffer (100 mM NaCl, 5 mM KCl and 5 mM $MgCl_2$, pH 7.4).

All other chemical agents were purchased from Sigma-Aldrich (USA) and Sinopharm Chemical Reagent Beijing Co., Ltd. Ultrapure water with electric resistance >18 M Ω was supplied from a Millipore Milli-Q water purification system (Billerica, MA, USA).

2.2 Telomerase Extracts

The commercial TRAPeze telomerase detection kit S7700 was purchased from Millipore and was used to provide telomerase-positive cells and a TRAP control group result. The telomerase was extracted from positive control cells (10^6 cells) from the S7700 kit. The cells were broken down by 200 μ L of 1 \times CHAPS Lysis Buffer, whose sediment was removed by centrifugation (12,000 rpm, 20 min); next, 160 μ L of liquid supernatant was repacked as 10 μ L of mother liquor and stored at -86°C. Before being used, the mother liquor was 20 \times diluted by 1 \times CHAPS Lysis Buffer, generating 250 cells- μ L⁻¹ of telomerase extracts.

2.3 Preparation of Oligonucleotide-adsorbing GO Probes

Telomeric primer P2 was first incubated in a mixed solution for 18 hrs. The mixed solution contain 1 μL of dNTP, 1 μL 50 $\mu\text{mol}\cdot\text{L}^{-1}$ of P2 DNA, 5 μL of 10 \times TRAP Reaction Buffer, 2 μL of different quantities of telomerase cell extracts (1, 5, 10, 50, 100, 500 cells and 500 cells heat-treated at 95°C for 10 min), and a number of PCR-Grade Water to bring the total volume to 50 μL . The incubated products were then mixed with fluorescent probe P1 and GO at various concentrations (1 $\text{mg}\cdot\text{mL}^{-1}$, 0.5 $\text{mg}\cdot\text{mL}^{-1}$, 0.2 $\text{mg}\cdot\text{mL}^{-1}$, 0.1 $\text{mg}\cdot\text{mL}^{-1}$) to achieve a final concentration of 50 nM DNA in each solution for 30 min at room temperature.

2.4 Apparatus

Atomic force microscopy (AFM) was conducted using an SPA400 equipped with an SPI3800N controller microscope instrument (Seiko Instruments Inc., Japan) in tapping mode to simultaneously collect the height and phase data from GO. The XPS spectrum of GO was measured using an Axis Ultra (Kratos Analytical Ltd., Japan), and the Raman spectrum was collected on a Renishaw inVia system (Renishaw, UK).

The fluorescence profiles of the DNA probe and primer mixtures were obtained using a Hitachi F-4500 fluorometer (Hitachi Co. Ltd., Japan) with an excitation wavelength of 480 nm.

PCR was carried out in a Mastercycler (Eppendorf Co. Ltd., Germany). Electrophoresis was performed in a Hoefer Minive (Pharmacia Biotech, Japan) and was used for the detection of PCR products in order to compare our method with TRAP. SYBR Green I used in electrophoresis was purchased from Invitrogen Ltd, while Taq DNA Polymerase ET101 (5 unit/ μL) and DNA Ladder Marker MD100 were purchased from Tiangen Biotech (Beijing) Co., Ltd.

2.5 Characterisation of Go

An AFM image and XPS spectra of the synthesised GO are shown in Fig. 1. It can be seen that the GO sheet size was less than 1 μm , with a height of 1.19 ± 0.11 nm, demonstrating that the GO is a single-layer carbon material. The GO was also characterised by Raman. (See Fig. S-1 of supplementary Data for more details).

XPS is a powerful surface technique that can provide information about the state and environment of atoms in a sample. The C1s core level of XPS has been used to distinguish sp^2 and sp^3 hybridisation in carbon nanomaterials [40]. The C1s XPS spectrum of GO clearly indicates a considerable degree of oxidation with three components that correspond to carbon atoms in different functional groups [41]: the non-oxygenated ring C (284.80 eV, sp^2 hybridised), the C in C–O bonds (287.01 eV), and the carbonyl C (288.62 eV). D and G bands of GO were found in the Raman spectrum (See Fig. S-1 of supplementary Data). The D band at 1320 cm^{-1} arises from sp^3 -hybridised carbon, and the peak at 1602 cm^{-1} represents the E_{2g} zone centre mode of the crystalline graphite [42]. There was also a 2D band at 2600 cm^{-1} . The relative intensity ratio of the D and G lines (I_D/I_G ratio) was 1.005, which was proportional to the number of defect sites in graphite carbon. All the information above indicated that these graphite materials were GO sheets with significant edge-plane-like defective sites on the surface [43-46].

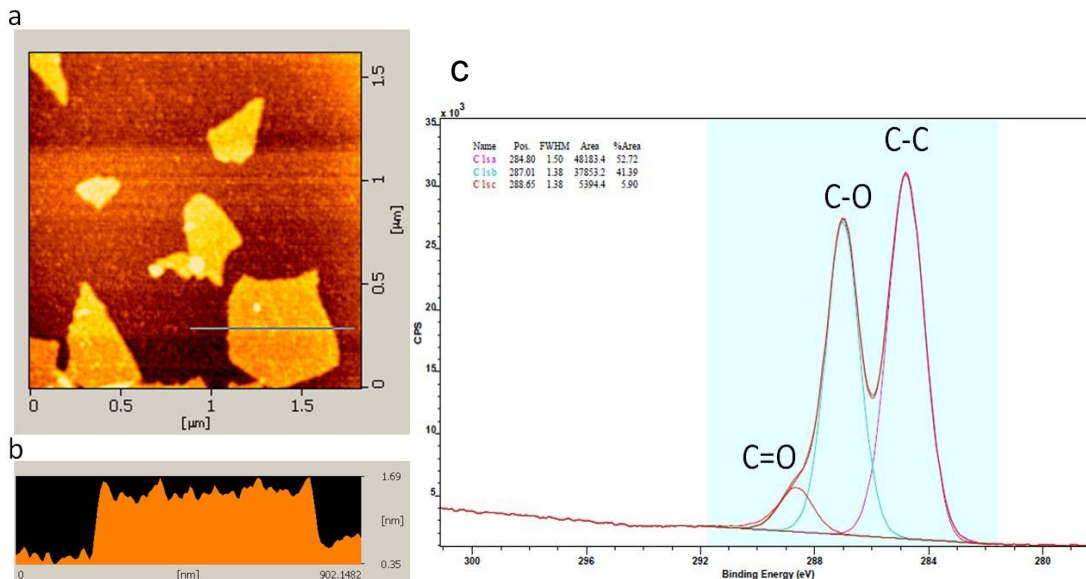


Fig. 1. (a) AFM image of GO on mica; (b) the cross-sectional profile of the AFM image along the black line; (c) XPS spectra of GO, shows the C-C bond, C-O bond and C=O bond

3. RESULTS AND DISCUSSION

3.1 Fluorescence Emission Spectra of Different Mixed Systems

Fig. 2 displays the fluorescence emission spectra of different mixed systems for $0.5 \text{ mg}\cdot\text{mL}^{-1}$ GO. Spectrum a is the fluorescence emission of the P1 probe itself, while spectrum b shows that GO can totally quench the fluorescence of P1. Spectrum c indicates that the P2 primer can enhance the fluorescence of the P1 probe by diluting the concentration of P1 and reducing the probe's self-quenching effect. Spectra d and e show that GO can also quench the ssDNA probe's fluorescence in the presence of P2 primer or cell extracts (telomerase) separately. These results suggest that these two elements were both necessary for fluorescence recovery in the mixture solution. Even in the presence of P2 primer after incubation with inactivated 500-cell extracts, as spectrum f shows, the system's fluorescence was still quite weak. Only when P2 primers were incubated with 500-cell extracts, the P1 probe could be hybridised with the extended primer forming a dsDNA and released from the GO surface, resulting in a high fluorescence signal (Fig. 2. line g). The experiment described above can clearly distinguish differences in telomerase activity based on fluorescence recovery levels.

This PCR-free method harnesses the special oligonucleotide-adsorption properties of GO by employing fluorescent ssDNA P1 as an analysis probe. This probe was adsorbed in the presence of GO because of the π - π stacking interaction between the ring structures in nucleobases and the hexagonal cells of graphene, which lead to the fluorescence quenching of ssDNA P1 and exhibited minimal background fluorescence. In contrast, when the primer DNA P2 was extended by telomerase in cell extracts after incubation and added to the probe solution, strong emission was observed attributed to the hybridization of extended primer DNA P2 and P1 probe which was released from the GO (see Scheme.

1, ②). In other experimental conditions, for example, without incubation of cell extracts or incubation with inactivated telomerase at 95°C, fluorescence emission was weak (see Scheme. 1, ①). Therefore, only when P2 primer was extended by active telomerase and hybridize with P1 probe to a double-helix DNA and that broke away from the surface of GO, which gives rise to the strong fluorescence. The quenching of fluorescence from the P1 probe by GO in the absence of telomerase provides a high signal-to-background ratio for telomerase activity detection.

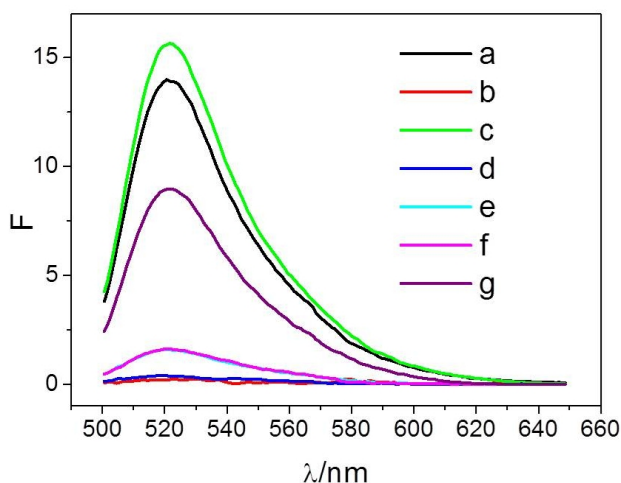
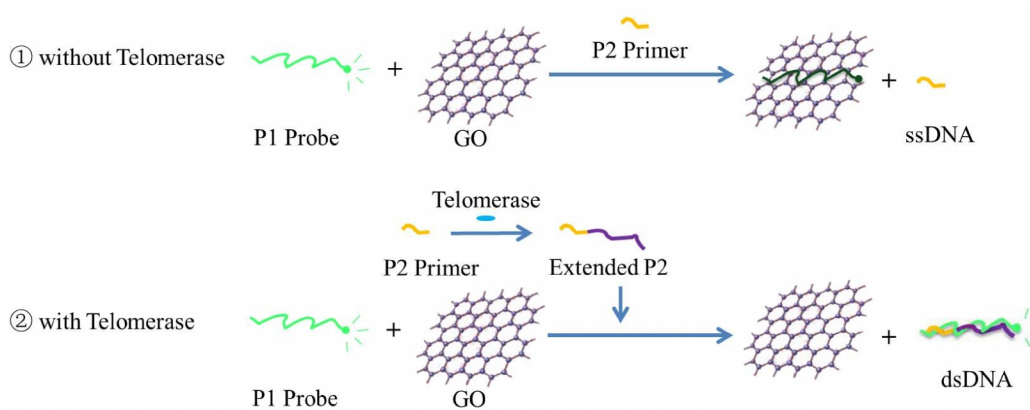


Fig. 2. Fluorescence emissions of FAM of 50 nM P1 DNA in different systems
 line a: only P1 DNA; line b: P1 and GO; line c: P1 and P2 DNA; line d: P1 with 500 cell extracts and GO; line e: P1, P2 DNA and GO; line f: P1 and P2 incubated with inactivated 500 cell extracts for 18 hrs and GO; line g: P1 and P2 incubated with 500 cell extracts for 18 hrs and GO. The excitation wavelength was 480 nm



Scheme 1. Illustration of the GO-based fluorescence method for telomerase activity detection. ①: DNA P1 probe fluorescence emission was weak in the situation primer P2 without incubation of cell extracts or incubation with inactivated telomerase at 95°C; ②: When primer P2 was extended by telomerase in cell extracts after incubation and added to the P1 probe solution, strong emission was observed

3.2 Telomerase-activity Assay Under Different GO Concentrations

In order to find suitable experimental conditions for telomerase activity detection, we tested various GO concentrations, including $1 \text{ mg}\cdot\text{mL}^{-1}$, $0.5 \text{ mg}\cdot\text{mL}^{-1}$, $0.2 \text{ mg}\cdot\text{mL}^{-1}$ and $0.1 \text{ mg}\cdot\text{mL}^{-1}$. Adsorption and quenching efficiency varied under these different concentrations, as exhibited in the fluorescence spectra from the P1+P2+GO mixtures. The normalised fluorescence factor f is introduced to support the discussion of telomerase-activity detectability under different GO concentrations.

$$f = (F_x - F_{P1+P2+GO}) / (F_{P1+P2} - F_{P1+P2+GO}) \quad (1)$$

This factor is defined by equation 1, in which F_x is the fluorescence emission of P1 DNA and P2 primers incubated with specific concentrations of cell extracts at specific GO concentrations; $F_{P1+P2+GO}$ is the fluorescence background of P1, P2 DNA at specific concentrations of GO and F_{P1+P2} is the fluorescence emission of P1 and P2 DNA. After such normalisation, the detection of telomerase activity using this GO-based fluorescence method can be compared at different GO concentrations.

Fluorescence signals were collected while systematically varying GO and telomerase concentrations (See Fig. S-2 in supplementary Data). For example, at a $0.2 \text{ mg}\cdot\text{mL}^{-1}$ GO concentration, fluorescence signals were collected after incubating P2 primer with telomerase extracted from between 1 and 500 cells (Fig. 3). Fig. 4(a) shows the work curves of different GO concentrations in the f - Log(cell number) diagram, demonstrating that $0.5 \text{ mg}\cdot\text{mL}^{-1}$ and $0.2 \text{ mg}\cdot\text{mL}^{-1}$ were appropriate GO concentrations. Generally, fluorescence signals were low when the GO concentration was too high (such as $1 \text{ mg}\cdot\text{mL}^{-1}$) because of the strong quenching effect. Conversely, the fluorescence background was too high when the GO concentration was low (such as $0.1 \text{ mg}\cdot\text{mL}^{-1}$), generating measuring errors for telomerase activity detection. When the GO concentration was in between these two extremes (such as $0.5 \text{ mg}\cdot\text{mL}^{-1}$ and $0.2 \text{ mg}\cdot\text{mL}^{-1}$), better and linear working curves were obtained. Table 1 displays the slopes and R^2 of the work curves at different GO concentrations. Moreover, inactivated telomerase comparisons were carried out at each GO concentration, as seen in Fig. 4 (b). After 10 min of 95°C heat inactivation, telomerase is unable to extend telomeric primer P2 and the weak fluorescence signals of P1 can be easily distinguished from activated telomerase.

3.3 Control Experiment

To understand the role of GO in this telomerase activity detection method, control studies were carried out in the absence of GO. As seen in Fig. 5 in the supporting information, normalised fluorescence curves at different telomerase concentrations were nearly the same, demonstrating that GO was the critical element in our fluorescence method. This effect is attributed to distinction in adsorption between ssDNA and dsDNA, which amplify differences in the fluorescence signal before and after telomeric extension and result in a high signal/background ratio. We conclude that this GO-based fluorescence method for telomerase activity detection provides the best results at $0.5 \text{ mg}\cdot\text{mL}^{-1}$ or $0.2 \text{ mg}\cdot\text{mL}^{-1}$ GO concentrations. The detection limits of this assay were 50 cells and 5 cells for $0.5 \text{ mg}\cdot\text{mL}^{-1}$ and $0.2 \text{ mg}\cdot\text{mL}^{-1}$, respectively, which is lower than that of the fluorescent QD method [20]. Though 1 cell could be detected at $0.1 \text{ mg}\cdot\text{mL}^{-1}$ GO concentration, further testing is needed due to the deviation from linearity.

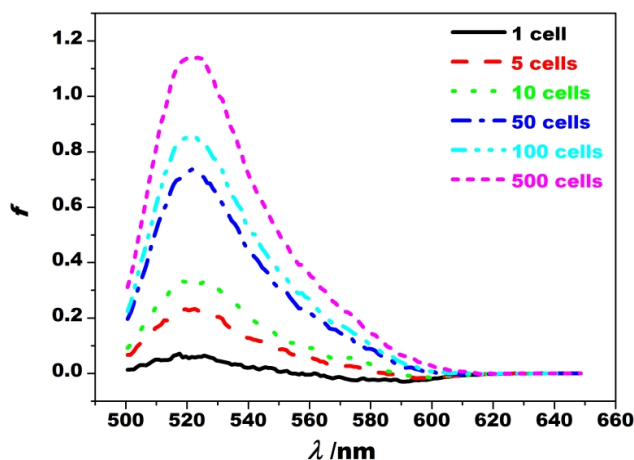


Fig. 3. Fluorescence factor f of P1 DNA with $0.5 \text{ mg}\cdot\text{mL}^{-1}$ GO and P2 primer incubated with various concentrations of telomerase (1, 5, 10, 50, 100, and 500-cell extracts). The excitation wavelength was 480 nm

Table 1. Slopes and R^2 of the calibration curves for telomerase activity detection at various GO concentrations

GO concentration/ $\text{mg}\cdot\text{mL}^{-1}$	Slope	R^2
1	0.0052	0.981
0.5	0.154	0.985
0.2	0.468	0.993
0.1	0.623	0.968

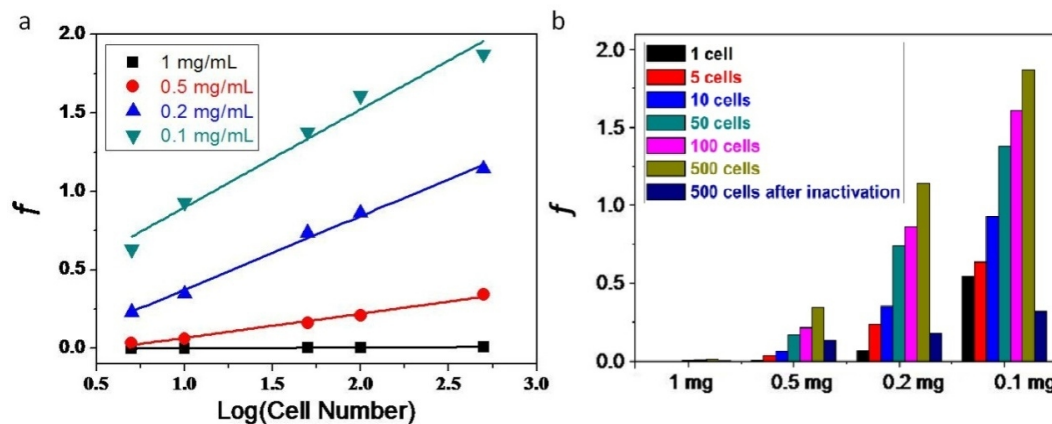


Fig. 4. Calibration curve for telomerase activity detection under different GO concentrations (a) and inactivated telomerase control (b). Square: $1 \text{ mg}\cdot\text{mL}^{-1}$, circle: $0.5 \text{ mg}\cdot\text{mL}^{-1}$, triangle: $0.2 \text{ mg}\cdot\text{mL}^{-1}$, inverse triangle: $0.1 \text{ mg}\cdot\text{mL}^{-1}$

Finally, we compared our assay to the TRAP method following the specifications of the S7700 kit. After PCR and electrophoresis, TRAP product bands were observed in the 500 cell extract lane and quantitation controls, while no products were observed in the

inactivated control and CHAPS control (for details, see Fig. S-3 in supplementary Data). The TRAP method requires 5 to 6 hours and has a detection limit of several hundred cells. Therefore, the need for more sensitive and convenient methods is still an important concern in the field of telomerase activity detection.

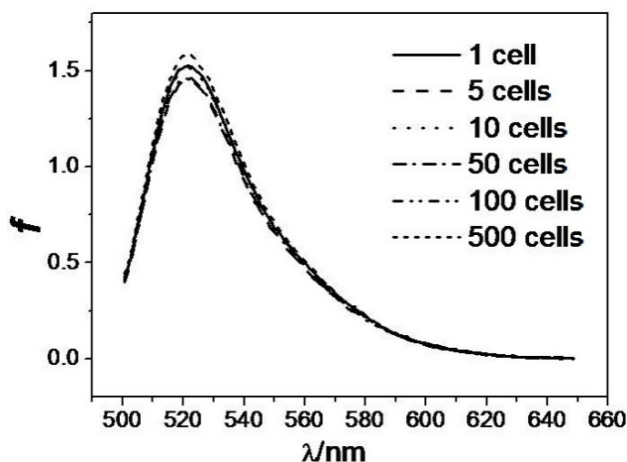


Fig. 5. Fluorescence factor f of control groups in the absence of GO

4. CONCLUSION

In summary, we have utilised the high fluorescence quenching ability of GO toward ssDNA to design a novel fluorescent sensor for multiplexed, ultra-sensitive and specific telomerase activity detection. This GO-based telomerase sensor has several advantages compared to the TRAP method. Principally, GO can be synthesised in large quantities and the DNA probe is only labeled with a single dye, reducing the cost for telomerase activity detection. Secondly, this method is PCR-free and easy to execute, which can avoid false positive results. Thirdly, GO-based detection improves sensitivity by quenching the fluorescence of the probe DNA, minimising the background fluorescence and resulting in an optimised detection limit of several-cell telomerase extracts. Although the telomeric primer extension in this method was time consuming, it is still highly promising due to its considerable sensitivity. Therefore, this GO-based method may provide opportunities to develop low cost and ultra-sensitive telomerase detection protocols using the conformational changes of DNA probes and the multi-functional nanomaterial GO. We expect that this will guide new research and enable important and widespread applications in many other areas of biological analysis.

SUPPLEMENTARY DATA

Supplementary data associated with this article can be found in the online version at:

<http://www.sciencedomain.org/download.php?f=Supplimentary462014IRJPAC12197.pdf&aid=5890>

COMPETING INTERESTS

Authors have declared that no competing interests exist.

REFERENCES

1. Greider CW, Blackburn EH. Identification of a specific telomere terminal transferase activity in tetrahymena extracts. *Cell*. 1985;43:405-413.
2. Zakian VA, Structure and function of telomeres. *Annu Rev Genet*. 1989;23:579-604.
3. Greider CW. Telomerase and senescence. *Bio Essays*. 1990;12:363-369.
4. Greider CW. Telomeres. *Curr Opin Cell Biol*. 1991;3: 444-451.
5. Perry PJ, Arnold JR, Jenkins TC. Telomerase inhibitors for the treatment of cancer: The Current Perspective, *Expert Opin Investig Drugs*. 2001;10:2141-2156.
6. Kim S, Kaminker P, Campisi J, Aging and Cancer. In *Search of a Happy Ending*, *Oncogene*. 2002;21:503-511.
7. Shay JW, Wright WE. Telomerase therapeutics for cancer: Challenges and New Directions. *Nat Rev Drug Discov*. 2006;5:577-584.
8. Morin GB. The human telomere terminal transferase enzyme is a Ribonucleoprotein that Synthesizes TTAGGG Repeats. *Cell*. 1989;59:521-529.
9. Kim NW, Platyszek MA, Prowse KR, Harley CB, West MD, Ho PLC, Coviello GM, Wright WE, Weinrich SL, Shay JW. Specific association of human telomerase activity with immortal cells and cancer. *Science*. 1994;266:2011-2015.
10. Lachey DB. A Homogeneous chemiluminescent assay for telomerase. *Anal Biochem*. 1998;263:57-61.
11. Tchirhov A, Rolhion C, Kemeny JL, Irthum B, Puget S, Khalil T, Chinot O, Kwiatkowski F, Pe´rresse BP, Vago P. Verrelle, clinical implications of quantitative real-time RT-PCR analysis of htert gene expression in human gliomas. *Br J Cancer*. 2003;88:516-520.
12. Nosek J, Rycovska A, Makhov AM, Griffith JD, Tomaska L. Amplification of telomeric arrays via rolling-circle mechanism. *J Bio Chem*. 2005;280:10840-10845.
13. Fajkus J. Detection of telomerase activity by the TRAP assay and its variants and alternatives. *Clinica Chimica Acta*. 2006;371:25-31.
14. Weizmann Y, Patolsky F, Katz E, Willner I. Magneto-mechanical detection of nucleic acids and telomerase activity in cancer cells. *Chem Bio Chem*. 2004;5:943-948.
15. Eskiocak U, Ozkan-Ariksoysal D, Ozsoz M, Öktem HA. Label-free detection of telomerase activity using guanine electrochemical oxidation signal. *Anal Chem*. 2007;79:8807-8811.
16. Freeman R, Sharon E, Teller C, Henning A, Tzfati Y, Willner I. DNAzyme activity of Hemin/Telomeric G-Quadruplexes for the optical analysis of telomerase and Its inhibitors. *Chem Bio Chem*. 2010;11:2362-2367.
17. Li Y, Li X, Ji XT, Li XM. Formation of G-quadruplex-hemin DNAzyme based on human telomere elongation and its application in telomerase activity detection. *Biosens Bioelectron*. 2011;26:4095-4098.
18. Pavlov V, Willner I, Dishon A, Kotler M. Amplified detection of telomerase activity using electrochemical and quartz crystal microbalance measurements. *Biosens Bioelectron*. 2004;20:1011-1021.
19. Maesawa C, Inaba T, Sato H, Iijima S, Ishida K, Terashima M, Sato R, Suzuki M, Yashima A, Ogasawara S, Oikawa H, Sato N, Saito K, Masuda T. A rapid biosensor chip assay for measuring of telomerase activity using surface plasmon resonance. *Nucleic Acids Res*. 2003;31:4.
20. Sharon E, Freeman R, Riskin M, Gil N, Tzfati Y, Willner I. Optical, electrical and surface plasmon resonance methods for detecting telomerase activity. *Anal Chem*. 2010;82:8390-8397.
21. Pavlov V, Xiao Y, Gill R, Dishon A, Kotler M, Willner I. Amplified chemiluminescence surface detection of DNA and telomerase activity using catalytic nucleic acid labels. *Anal Chem*. 2004;76:2152-2156.

22. Zhou X, Xing D, Zhu D, Jia L. Magnetic bead and nanoparticle based electrochemiluminescence amplification assay for direct and sensitive measuring of telomerase activity. *Anal Chem*. 2009;81:255-261.
23. Yang W, Zhu X, Liu Q, Lin Z, Qiu B, Chen G. Label-free detection of telomerase activity in hela cells using electrochemical impedance spectroscopy. *Chem Commun*. 2011;47:3129-3131.
24. Sato S, Kondo H, Nojima T, Takenaka S. Electrochemical telomerase assay with ferrocenylnaphthalene diimide as a tetraplex DNA-specific binder. *Anal Chem*. 2005;77:7304-7309.
25. Zheng G, Daniel WL, Mirkin CA. A new approach to amplified telomerase detection with polyvalent oligonucleotide nanoparticle conjugates. *J Am Chem Soc*. 2008;130:9644-9645.
26. Novoselov KS, Geim AK, Morozov SV, Jiang D, Zhang Y, Dubonos SV, Grigorieva IV, Firsov AA. Electric field effect in atomically thin carbon films. *Science*. 2004;306:666-669.
27. Schedin F, Geim AK, Morozov SV, Hill EW, Blake P, Katsnelson MI, Novoselov KS. Detection of individual gas molecules adsorbed on grapheme. *Nature Mater*. 2007;6:652-655.
28. Mohanty N, Berry V. Graphene-based single-bacterium resolution biodevice and DNA transistor: Interfacing graphene derivatives with nanoscale and microscale biocomponents. *Nano Lett*. 2008;8:4469-4476.
29. Wang Z, Zhou X, Zhang J, Boey F, Zhang H. direct electrochemical reduction of single-layer graphene oxide and subsequent functionalization with glucose oxidase. *J Phys Chem*. 2009;113:14071-14075.
30. Zhou Y, Bao Q, Tang LAL, Zhong Y, Loh KP. Hydrothermal dehydration for the "green" reduction of exfoliated graphene oxide to graphene and demonstration of tunable optical limiting properties. *Chem Mater*. 2009;21:2950-2956.
31. Tang Z, Wu H, Cort JR, Buchko GW, Zhang Y, Shao Y, Aksay IA, Liu J, Lin Y. Constraint of DNA on functionalized graphene improves its biostability and Specificit. *Small*. 2010;6:1205-1209.
32. Garaj S, Hubbard W, Reina A, Kong J, Branton D, Golovchenko JA. Graphene as a subnanometre trans-electrode membrane. *Nature*. 2010;467:190-194.
33. Lu CH, Yang HH, Zhu CL, Chen X, Chen GN. A graphene platform for sensing biomolecules. *Angew Chem*. 2009;121:4879-4881.
34. Wen Y, Xing F, He S, Song S, Wang L, Long Y, Li D, Fan C. A graphene-based fluorescent nanoprobe for Silver(I) ions detection by using graphene oxide and a silver-specific oligonucleotide. *Chem Commun*. 2010;46:2596-2598.
35. He SJ, Song B, Li D, Zhu C, Qi W, Wen Y, Wang L, Song S, Fang H, Fan C. A graphene nanoprobe for rapid, sensitive, and multicolor fluorescent DNA analysis. *Adv Funct Mater*. 2010;20:453-459.
36. Liu X, Aizen R, Freeman R, Yehezkeili O, Willner I. Multiplexed aptasensors and amplified DNA sensors using functionalized graphene oxide: Application for logic gate operations. *ACS Nano*. 2012;6:3553-3563.
37. Hummers W, Offeman J. Preparation of graphitic oxide. *J Am Chem Soc*. 1958;80:1339-1339.
38. Kovtyukhova NI, Ollivier PJ, Martin BR, Mallouk TE, Chizhik SA, Buzaneva EV, Gorchinskiy AD. Layer-by-layer assembly of ultrathin composite films from micron-sized graphite oxide sheets and polycations. *Chem Mater*. 1999;11:771-778.
39. Zhou M, Zhai Y, Dong S. Electrochemical sensing and biosensing platform based on chemically reduced graphene oxide. *Anal Chem*. 2009;81:5603-5613.

40. Díaz J, Paolicelli G, Ferrer S, Comin F. Separation of the sp^3 and sp^2 components in the C1s photoemission spectra of amorphous carbon films. *Phys Rev.* 1996;54:8064-8069.
41. Stankovich S, Dikin DA, Piner RD, Kohlhaas KA, Kleinhammes A, Jia Y, Wu Y, Nguyen ST, Ruoff RS. Synthesis of graphene-based nanosheets via chemical reduction of exfoliated graphite oxide. *Carbon.* 2007;45:1558-1565.
42. Tuinstra F, Koenig JL. Raman spectrum of graphite. *J Chem Phys.* 1970;53:1126-1130.
43. Zhou M, Wang Y, Zhai Y, Zhai J, Ren W, Wang F, Dong S. Controlled synthesis of large-area and patterned electrochemically reduced graphene oxide films. *Chem Eur J.* 2009;15:6116-6120.
44. Guo HL, Wang XF, Qian QY, Wang FB, Xia XH. A green approach to the synthesis of graphene nanosheets. *ACS Nano.* 2009;3:2653-2659.
45. Wang S, Ang PK, Wang Z, Tang ALL, Thong JTL, Loh KP. High mobility, printable, and solution-processed graphene electronics. *Nano Lett.* 2010;10:92-98.
46. Dreyer DR, Park S, Bielawski CW, Ruoff RS. The chemistry of graphene oxide. *Chem Soc Rev.* 2010;39:228-240.

© 2014 Zhu et al.; This is an Open Access article distributed under the terms of the Creative Commons Attribution License (<http://creativecommons.org/licenses/by/3.0>), which permits unrestricted use, distribution, and reproduction in any medium, provided the original work is properly cited.

Peer-review history:

The peer review history for this paper can be accessed here:

<http://www.sciencedomain.org/review-history.php?iid=536&id=7&aid=5890>